J Mater Sci (2010) 45:4073–4077
DOI 10.1007/s10853-010-4493-5

The mechanism of the failure of the dispersion-strengthened Cu–Al_2O_3 nanosystem

Michal Besterci · Oksana Velgosová · Jozef Ivan · Tibor Kvačkaj

Received: 26 December 2009 / Accepted: 6 April 2010 / Published online: 22 April 2010

Abstract The method of "in situ tensile testing in SEM" is suitable for investigations of fracture mechanisms because it enables to observe and document deformation processes directly, thank to which the initiation and development of plastic deformation and fracture can be reliably described. The deformation and fracture mechanisms of Cu–Al_2O_3 nanomaterials with 5 vol.% of Al_2O_3 phase has been analyzed using technique of the "in situ tensile testing in SEM." It has been shown that the deformation process causes break-up of large Al_2O_3 particles and decohesion of smaller ones. The final fracture path is influenced also by boundaries of nanograins, through which the principal crack propagates towards the sample exterior surface. Based on the experimental observations, a model of damage and/or fracture mechanisms has been proposed.

M. Besterci
Institute of Materials Research, Slovak Academy of Sciences, Watsonova 47, 043 53 Košice, Slovak Republic
e-mail: mbesterci@imr.saske.sk

O. Velgosová (✉)
Department of Non-ferrous Metals and Waste Treatment, Faculty of Metallurgy, Technical University, Letná 9/A, 04200 Košice, Slovak Republic
e-mail: oksana.velgosova@tuke.sk

J. Ivan
Institute of Materials and Machine Mechanics, Slovak Academy of Sciences, Račianska 75, 838 12 Bratislava, Slovak Republic
e-mail: ummsivan@savba.sk

T. Kvačkaj
Department of Metals Forming, Faculty of Metallurgy, Technical University, Vysokoškolská 4, 04200 Košice, Slovak Republic
e-mail: tibor.kvackaj@tuke.sk

Introduction

We have analyzed, as reported in [1–3] the fracture of Cu–Al_2O_3 and Cu–TiC systems by direct monitoring of the strain and fracture in a scanning electron microscope (SEM) (in situ tensile test in SEM). Both systems were prepared by different powder metallurgy technologies. The dispersed oxides and carbides in the matrix were not coherent. Differences in particle size and distribution caused differences in fracture mechanism, although both factures were ductile transcrystalline with dimples. Owing to the excellent high-temperature properties and sufficiently high values of electrical and thermal conductivity, the dispersion-strengthened Cu–Al_2O_3 materials, prepared by the methods of powder metallurgy, have found use as conductors in electrical machines employed at high temperatures, in contacts, in electrodes and in vacuum technique parts.

The aim of work is to analyze fracture mechanism in the Cu–Al_2O_3 nanocomposite system and to propose a damage model. The method of in situ tensile test in SEM was used for other materials, too [4–10].

Experimental materials and methods

Reaction milling and mechanical alloying was used to prepare the samples. Cu powder with the calculated addition of Al was homogenized by attrition in oxidizing atmosphere. The distribution of the obtained CuO was uniform. A subsequent treatment at 750 °C induced the reaction of CuO with the added Al powder, and led to the formation of Al_2O_3 particles. The remaining CuO was reduced by attrition in a mixture of $H_2 + H_2O$ (rate 1:100). The powder was compacted by cold pressing and hot extrusion at 750–800 °C.

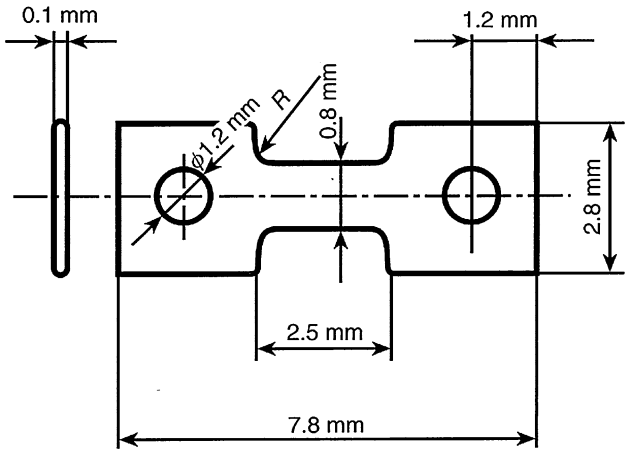

Fig. 1 The shape and dimension of a specimen

Microstructured material with 5 vol.% Al_2O_3 was transformed by the equal channel angular pressing (ECAP) method in two passes into a nanocomposite material. The experimental material was pressed through two right angled (90°) channels of a special die by route "C." The ECAP technology allows obtaining the very fine-grained microstructure–nanostructure by multiple pressings through the die.

This material with dimensions of ∅10 × 70 mm was deformed by the ECAP technique in two passes at room temperature in a hydraulic press in the equipment described in [11].

For the purposes of investigation, very small flat tensile test pieces, Fig. 1, with 0.15 mm thickness were prepared by electroerosive machining, keeping the loading direction identical to the direction of extrusion. They were ground and polished mechanically to a thickness of approximately 0.1 mm. The final operation consisted in double-sided final polishing of specimens with an ion thinning machine. The test pieces were fitted into special deformation grips inside the scanning electron microscope JEM 100 C, which enables direct observation and measurement of the deformation by ASID-4D equipment. From each one of the systems five samples were prepared.

Results and discussion

The microstructure of the starting material with 5 vol.% Al_2O_3 was fine-grained (the mean matrix grain size was 1 μm) Fig. 2, heterogeneous, with Al_2O_3 particles distributed in parallel rows as a consequence of extrusion and ECAP. The experimental materials were deformed at 20 °C at a strain rate of 6.6×10^{-4} s^{-1} in the elastic region. The replica is shown in Fig. 3, and diffractogram is shown in Fig. 4. Particles of size less than 0.25 μm were classified as

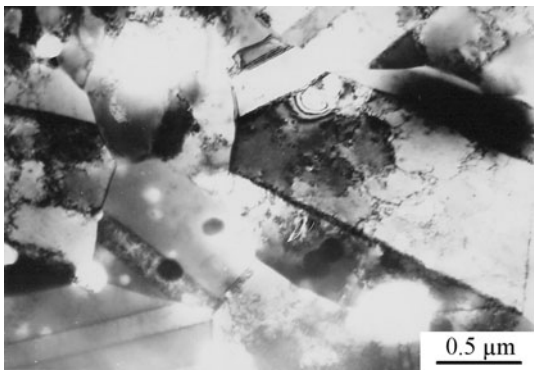

Fig. 2 The microstructure of the starting material

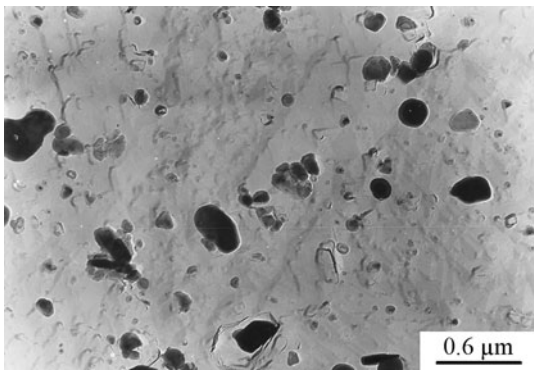

Fig. 3 Replica of material with 5 vol.% Al_2O_3

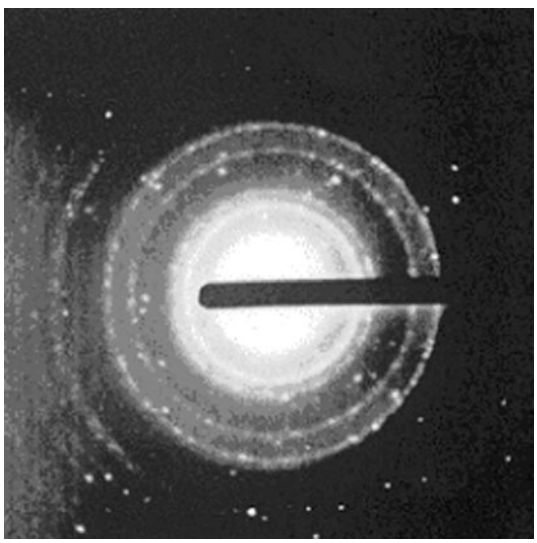

Fig. 4 Difractogram of Al_2O_3

effective dispersion particles of category A, and particles of size greater than 0.25 μm as particles of category B; the latter are ineffective from the point of view of strengthening; although they affect the deformation process and plastic properties. In addition to the particles mentioned,

the material also contained impurities, which were introduced during the preparation process of the material.

The material after ECAP is on the border of nanostructured materials. The TEM micrographs, Fig. 5, showed that the mean grain size was 100–200 nm, small amount of dislocations are present in nanograins, too, but mostly on the boundaries. The nanostructure formation takes place most probably by a three-stage mechanism, described in [12–14]. This model has been experimentally verified only for several specific materials but in our case it seems to be probably usable. The model includes creation of cell structure, then formation of transitory cell nanostructure with large angle disorientation, and finally formation of nanostructured grains with size of $\sim$100 nm. However, here one has to consider the retarding effect due to present dispersoid particles.

Deformation process of the loaded layer causes fracture of large, B-type, particles in the middle of the specimen (Fig. 6), which initializes fracture path roughly perpendicular to the loading direction. The fracture path is determined also by decohesion of smaller particles (type A) (Fig. 7). Since the volume fractions of Al_2O_3 particles are small, their distribution in lines does not influence the trajectory of fracture, which has low relative deformation $\varepsilon = 0.1$. Unlike the microstructured Cu-based composites, in this case, it has been shown that the nanograin boundaries play an important role. In the final phase (Fig. 8), a crack propagates along the nanograin boundaries, which has been observed experimentally on the crack line

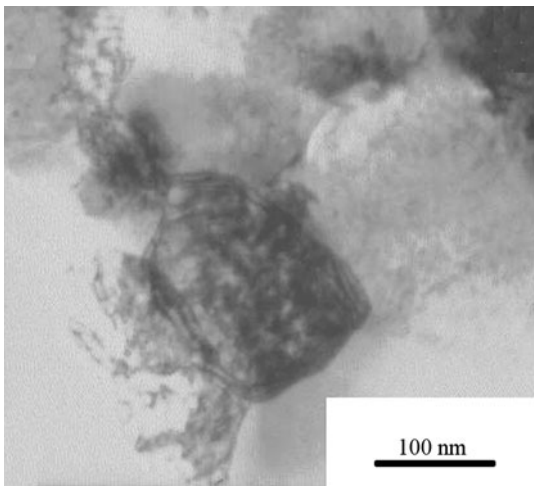

Fig. 5 The TEM micrographs of the material after ECAP

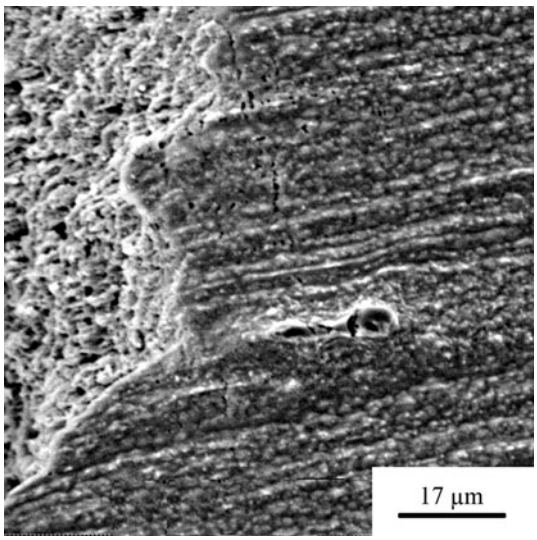

Fig. 7 Decohesion of smaller particles category A

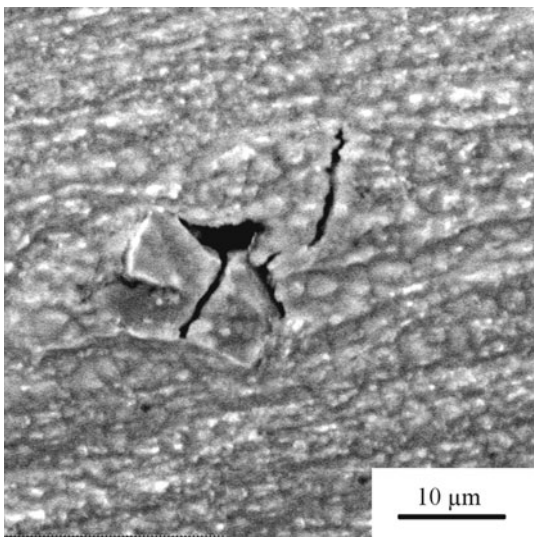

Fig. 6 Fracture of large (B) Al_2O_3 particles in the middle of the layer

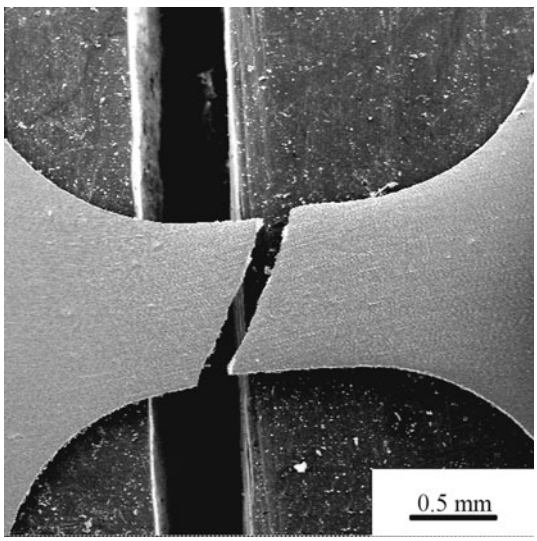

Fig. 8 The final phase of the crack

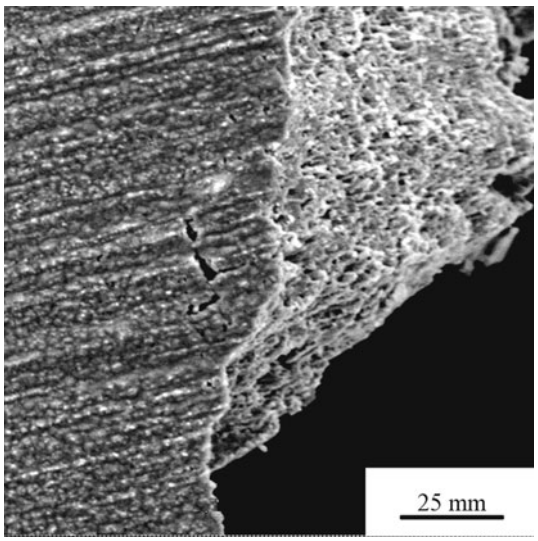

Fig. 9 Surface morphology (dimples) of the material with 5 vol.% Al_2O_3

(profile), and it is documented also by the ductile fracture surface with typical dimples in Fig. 9.

A detailed study of the deformation changes showed that the crack initiation was caused by decohesion, and occasionally also by rupture of the large particles. Decohesion is a result of different physical properties of different phases of the system. The Cu matrix has significantly higher thermal expansion coefficient and lower elastic modulus ($\alpha = 17.0 \times 10^{-6}\ K^{-1}$, $E = 129.8$ GPa) than Al_2O_3 ($\alpha = 8.3 \times 10^{-6}\ K^{-1}$ and $E = 393$ GPa). Large differences in the thermal expansion coefficients result in high stress gradients, which arise on the interphase boundaries during the hot extrusion. Since $\alpha_{matrix} > \alpha_{particle}$, high compressive stresses can be expected. However, because the stress gradients arise due to the temperature changes, during cooling (which results in increase of the stress peaks) their partial relaxation can occur. Superposition of the external load and the internal stresses can initiate cracking at interphase boundaries. This is in accordance also with the dislocation theories, which argue that the particles in composite may cause an increase in the dislocation density as a result of thermal strain mismatch between the ceramic particles and the matrix during preparation and/or thermal treatment. In our case, the coefficient of thermal expansion of the matrix is much higher than that of the secondary particles and the resulting thermal tension may relax around the matrix–particle interfaces by emitting dislocations, whose density can be calculated according to procedure described in [15].

Based on the microstructure changes observed in the process of deformation, the following model of fracture mechanism is proposed (Fig. 10a–d).

(a) The microstructure in the initial state is characterized by Al_2O_3 particles, categorized as B.

(b) With increasing tensile load, local cracks, predominantly on specimen side surfaces, are formed by decohesion of smaller A particles.

(c,d) In further increasing deformation of nanocomposite materials, the nanograin boundaries start to play an important role. Since the volume fraction of these boundaries is high and the size of the B and A particles is equal to the matrix grain size, crack propagates preferentially along the nanograin boundaries in a 45° angle.

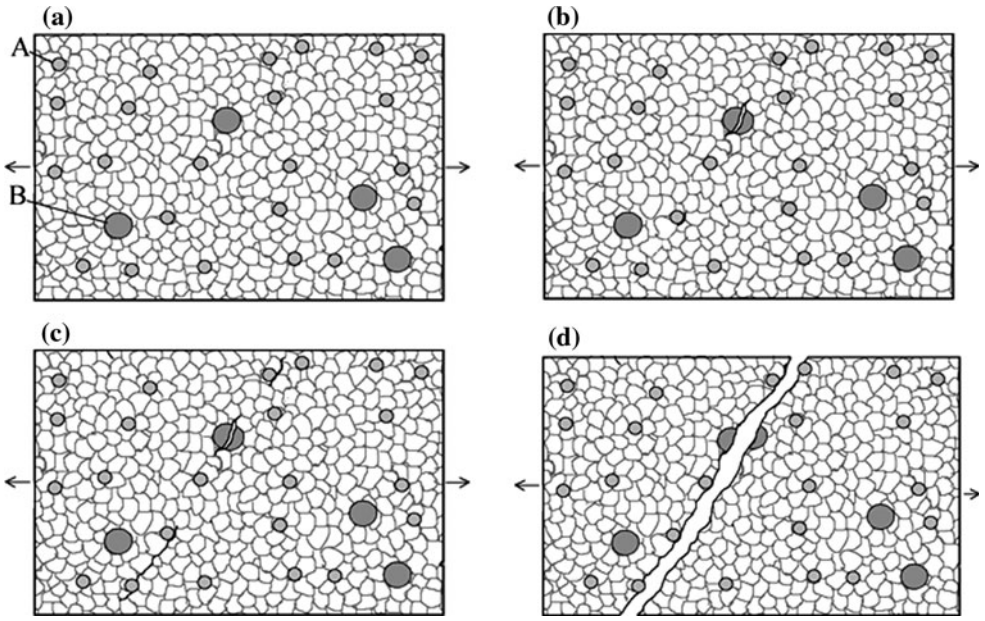

Fig. 10 **a–d** Model of the fracture mechanism

Conclusion

The aim of the study was to evaluate the influence of volume fraction of Al_2O_3 (5 vol.%) particles on the fracture mechanism by means of the method "in situ tensile test in SEM."

Based on the microstructure changes obtained in the process of deformation of the dispersion strengthened Cu–Al_2O_3 alloys, a model of fracture mechanism was proposed. With increasing tensile load, the local cracks, predominantly on specimen's side surfaces, are formed by rupture of large B and decohesion of smaller A particles. The orientation of cracks tends to be perpendicular to the loading direction, depending on the particle volume fraction. The final rupture, i.e., interconnection of the side cracks along the loading direction, takes place at nanograin boundaries, depending on the volume fractions of oxide (Al_2O_3) particles in a 45° angle.

Acknowledgement The work was supported by the Slovak National Grant Agency under the Project VEGA 2/0105/08.

References

1. Besterci M, Ivan J (1997) Kovove Mater 35:278
2. Besterci M, Ivan J, Kovac L, Weissgaerber T, Sauer C (1998) Kovove Mater 36:239
3. Besterci M, Ivan J, Kovac L (2000) Mater Lett 46:181
4. Besterci M, Ivan J (1996) J Mater Sci Lett 15:2071
5. Besterci M, Ivan J (1998) J Mater Sci Lett 17:773
6. Besterci M, Ivan J, Kovac L (2000) Kovove Mater 38:21
7. Besterci M, Ivan J, Velgosová O, Pešek L (2001) Kovove Mater 39:361
8. Besterci M, Velgosová O, Ivan J, Hvizdoš P, Kohútek I (2008) Kovove Mater 46:139
9. Mocelin A, Fougerest F, Gobin PF (1993) J Mater Sci 28:4855. doi:10.1007/BF00361147
10. Velísek R, Ivan J (1994) Kovove Mater 32:531
11. Besterci M, Velgosová O, Ivan J, Hvizdoš P, Kvačkaj T (2009) Kovove Mater 47:221
12. Valiev RZ, Alexandrov IV (2000) Nanostrukturnyje materialy polučennyje intensivnoj plastičeskoj deformaciej. Logos, Moskva
13. Valiev RZ (2003) In: Senkov ON, Miracle DB, Firstov SA (eds) Proceedings of metallic materials with high structural efficiency. NATO Science Series, Kijev. IOS Press, Amsterdam and Kluwer Acad. Publishers, Dordrecht, p 79
14. Valiev RZ (1995) Nanostruct Mater 6:73
15. Lukáč P, Trojanová Z (2006) Kovove Mater 44:243